JOURNAL OF MATERIALS SCIENCE **38** (2003) 4567–4571

Mechanical properties of reaction sintered TiN ceramics with B_4C addition

K. WANG, V. D. KRSTIC
Centre for Manufacturing of Advanced Ceramics and Nanomaterials, Queen's University, Nicol Hall, Kingston, Ontario, Canada
E-mail: krstiev@post.queensu.ca

Reaction sintering of TiN with B_4C addition was developed to densify the composite without the application of external pressure. The process utilizes high affinity of B for Ti which leads to the formation of extremely fine highly active TiB_2. The addition of 6–8 wt% B_4C is sufficient to increase the sintered density to over 96% theoretical density, fracture toughness to 3.5 MPa·$m^{1/2}$, flexural strength to 415 MPa, and hardness to ~14 GPa. The major toughening mechanism was identified to be the crack deflection caused by the presence of hard and tough TiB_2 particles. The large improvements in mechanical properties make this *in situ* produced composite viable material for applications requiring higher level of reliability.

1. Introduction

For many years, the TiN has been successfully used as protective coating for a range of materials [1] including cemented carbide tool inserts, tool steel, and ceramics. The coating not only provides increased hardness and wear resistance but also prevents reaction of the tool with the metal work piece at high temperature normally generated in the course of machining. Despite extensive application of TiN as coatings, the use of this ceramic in a bulk form has been limited, mainly due to poor sinterability and inherent brittleness. So far, all sintering of TiN has been done with the help of external pressure, either hot- or hot-isostatic pressing. Without the use of sintering aids even the application of external pressure could not produce densities higher than 96% theoretical density (TD) [2]. Recently, however, it has been discovered that the reaction sintering with B_4C as an additive can greatly increase the driving force for sintering and allow the consolidation of the bulk TiN to densities in excess of 96%TD at temperatures of 2000°C [3]. Furthermore, the presence of *in situ* formed uniformly distributed TiB_2 particles have potential of impeding the crack propagation and enhancing fracture toughness and strength.

The objective of this paper is to systematically study the effect of B_4C addition on mechanical properties of pressureless sintered TiN and to elucidate the mechanism of strengthening and toughening.

2. Experimental

Submicron size TiN and B_4C powders (both manufactured by H.C. Starck Co.) were used as raw materials. The initial powders were mixed by ball milling for 8 h in a plastic jar using ZrO_2 balls as a milling media and methanol as a vehicle. To increase the green density and strength, polyethylene glycol was used as binder and lubricant. The mixed powders were dried at 80°C for 4 h, followed by mechanical pressing into pellets with dimensions 35 mm × 16 mm × 7 mm. The mechanically pressed samples were then encapsulated in plastic bags and isostatically pressed at a pressure of 225 MPa. Sintering was done in a vacuum resistant furnace with graphite as heating elements at temperature ranging from 1980 to 2020°C for 1 h. The detailed sintering protocol is given in the separate publication [3]. The density of sintered samples was measured using the water displacement method with distilled water as the immersion medium.

The pressureless sintered materials were cut and polished and then thermally etched at 1460°C under vacuum of 10^{-2}–10^{-3} mmHg. The microstructure was observed by scanning electron microscopy (SEM).

The phase identification was done from X-ray diffraction, using Cu_{Ka} radiation, on polished samples from the relative intensities of all peaks. Fracture toughness (K_{IC}) and Vickers hardness (H_V) were measured by indentation technique. The following equation, proposed by Evans and Charles [4], was used for toughness determination:

$$K_c = 0.016P\sqrt{\frac{Ec^3}{H_V}} \quad (1)$$

where P is the load, E is the Young's modulus, H_V is the Vickers hardness, and c is the half-length of the radial crack. Bend tests were performed at room temperature on rectangular samples (32 mm × 17 mm × 7 mm) using the four-point bend jig with inner span of 13.27 mm and an outer span of 23.88 mm, and cross-head speed of 0.003 mm/s.

3. Results

3.1. Reaction mechanism and microstructure development

The change of sintered density of TiN as a function of B_4C addition is shown in Fig. 1. Even small addition of B_4C was enough to achieve densities of over 95% TD without the application of external pressure. Clearly, the system possesses greatly increased driving force for sintering compared to TiN without B_4C addition. The increased driving force for sintering comes from the presence of very fine, highly active TiB_2 particles formed in the course of the reaction:

$$(2+4x)\mathrm{TiN} + 2x\mathrm{B_4C} = 2\mathrm{Ti}(\mathrm{C}_x\mathrm{N}_y) + 4x\mathrm{TiB_2} + (2x-y+1)\mathrm{N_2}\uparrow \quad (2)$$

The temperature at which the reaction (2) is in equilibrium was calculated to be $T = 1115^\circ$C [3]. To validate this prediction, a set of samples containing 8 wt% B_4C was heated up to temperatures ranging from 1400 to 1550°C and held for 60 min. The X-ray analysis showed that the reaction starts before 1450°C and is complete at approximately 1500°C [3]. The X-ray data also show that the carbon component introduced into the system via B_4C addition dissolves into the TiN lattice without forming a separate phase. The result of reaction (2) is the composite consisting of TiN matrix and very fine uniformly distributed TiB_2 particles. Based on the reaction (2), the volume fraction of the TiB_2 phase is directly related to the level of B_4C added.

Due to a large difference in densities between TiB_2 ($\rho = 4.91$ g/cm^3) and B_4C ($\rho = 2.52$ g/cm^3) for each percent of B_4C added to TiN there will be approximately 2.5% TiB_2 formed during the reaction (Table I). For example, the addition of only 6 wt% B_4C results in the formation of ~15.82 wt% TiB_2.

The presence of TiB_2 particles in the TiN matrix plays two important roles. One is to pin the grain boundaries during sintering and limit their mobility. This role is important in that it allows the diffusion to take place along the grain boundaries rather then through the lattice and thus provide easy diffusion paths. The other role of TiB_2 is to impart higher resistance to crack propagation and enhance mechanical properties of the composite.

TABLE I Volume fraction of TiB_2 for different B_4C additions

	Green			Sintered		
Specimen	TiN (wt%)	B_4C (wt%)	V_f (B_4C) (vol%)	$Ti(C_{1-x}N_x)$ (wt%)	TiB_2 (wt%)	V_f (TiB_2) (vol%)
TNBC05	99.5	0.5	1.06	98.74	1.26	1.50
TNBC2	98	2	4.18	94.89	5.11	6.02
TNBC4	96	4	8.18	89.62	10.38	12.1
TNBC6	94	6	12.01	84.18	15.82	18.2
TNBC8	92	8	15.68	78.56	21.44	24.3
TNBC10	90	10	19.20	72.76	27.24	30.50

As shown in Fig. 1, the addition of B_4C increases the sintered density of TiN for all concentrations of B_4C of up to ~4 wt%. Further increase of B_4C addition above ~4 wt% leads to a rapid decrease in sintered density reaching a value of only 85% TD at 10 wt% B_4C. This large decrease in density with B_4C addition is associated with high level of porosity in the green compact created as a result of reaction between TiN and B_4C which takes place prior to sintering. Density measurements of the green compact after heat treatment at 1550°C for 60 min, which is the temperature at which the conversion of B_4C to TiB_2 is complete, revealed much higher level of porosity in samples with 6–10 wt% B_4C compared to samples with 0.5–4 wt% B_4C. This additional porosity is created by the consumption of TiN component and the loss of N_2 gas in accordance with reaction (2). The creation of porosity is further intensified by the replacement of lower density B_4C additive to higher density TiB_2 particles. At lower levels of B_4C addition (<~4 wt%), the level of porosity created by the reaction (2) is low and the driving force for sintering is high due to the presence of extremely fine high surface area TiB_2 particles. Under this condition high sintered densities are achieved. At higher levels of addition, above approximately 6 wt%, the porosity created as a result of reaction is so high that it cannot be eliminated during sintering, resulting in lower densities.

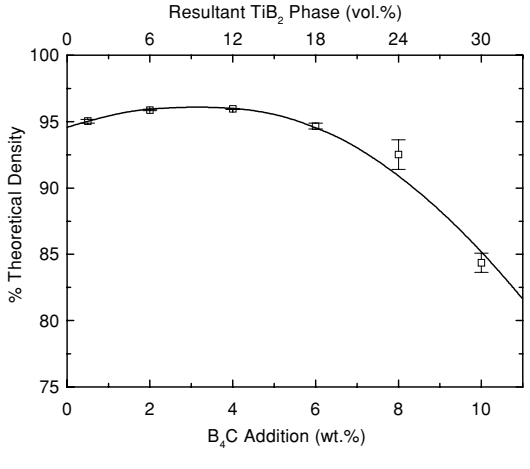

Figure 1 Changes of relative density with boron carbide addition. Samples were held at 1550°C for 60 min before sintered at 2000°C for 60 min.

3.2. Mechanical properties

As described in Section 3.1, the presence of TiB_2 particles serves to lower the grain boundary mobility and increase the sintered density. Their presence also influences the mechanical properties of the sintered samples including fracture toughness, flexural strength and Vickers hardness. The change of fracture toughness with volume fraction of TiB_2 particle is given in Fig. 2. The highest fracture toughness was achieved in samples with 7–8 wt% B_4C addition, which is equivalent to 20–24 vol% TiB_2. A sharp decrease in toughness was observed for samples containing B_4C additions above ~8 wt% (>24 vol%). There are several factors which can affect the fracture toughness. One is the residual stress and the attendant microcracking which occurs as a result of thermal expansion mismatch between TiN matrix and TiB_2 particles [5]. On cooling from

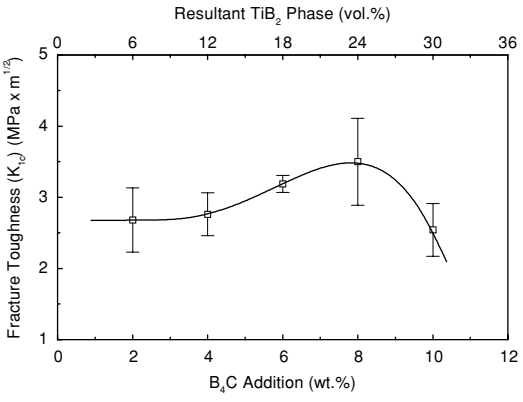

Figure 2 Change of fracture toughness with B_4C addition.

the fabrication temperature, the difference in the coefficients of thermal expansion between TiN ($\alpha = 9.35 \times 10^{-6}/^{\circ}C$) and TiB_2 ($\alpha = 8.7 \times 10^{-6}/^{\circ}C$) can lead to the development of residual stress. Assuming that the temperature at which the relaxation of residual stress becomes negligible is 800°C, and substituting values for $\nu_{TiN} = \nu_{TiB_2} = 0.2$, $E_{TiN} = 251$ GPa and $E_{TiB_2} = 530$ GPa in equation [6]

$$\sigma = \Delta\alpha\Delta T \Big/ \left\{(1-\nu_{TiN})/2E_{TiN} + \left(1-2\nu_{TiB_2}\right)/E_{TiB_2}\right\} \quad (3)$$

gives the residual stress of 132 MPa. This stress will interact with the propagating crack tip stress field and force the crack to move toward the particle-matrix interface. Once the crack reaches the particle, it can move along the particle matrix interface, through the particle, or in the matrix, depending on the fracture toughness/strength of the particular, grain boundary phase and TiN phase. Fig. 3 shows the path of crack propagation in samples containing ~12 and 24 vol% TiB_2 particles. Inspection of Fig. 3a indicates that the crack is attracted to the TiB_2 particle but it does not propagate through it. Rather, it moves mostly along the particle-matrix interface, suggesting the existence of weak

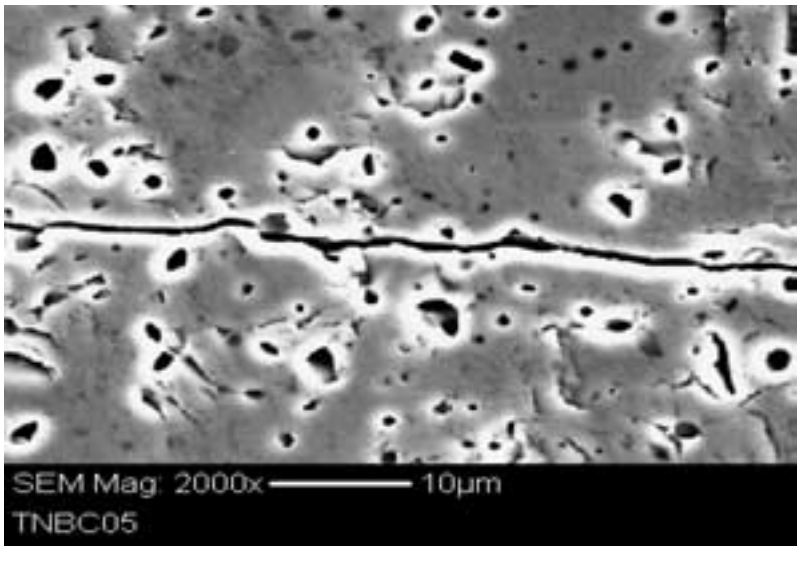

(a)

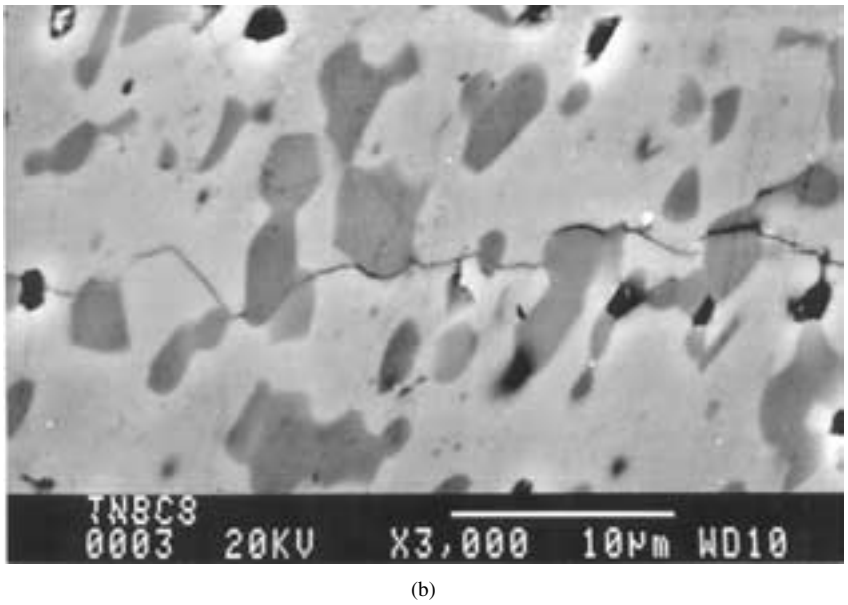

(b)

Figure 3 Crack paths in samples containing 4 wt% B_4C (a), and samples containing 8 wt% B_4C addition (24 vol% TiB_2). Note much larger crack deflection in samples with larger size and number of TiB_2 particles (sample b).

interface. This change of crack direction during its propagation contributes to toughening and strengthening of the resultant composite. The level of toughening depends on the TiB_2 particle size and its volume fraction. As the volume fraction and the size of TiB_2 are increased the deflection of crack also increase, leading to the raise in fracture toughness. The highest fracture toughness is obtained for the samples with sufficiently large particle volume fraction (∼24%) and a moderate level of porosity. At lower levels of additions (<6–8 wt%), the porosity is small and its effect on fracture toughness is also small. At B_4C additions of ∼4 wt%, which corresponds to TiB_2 volume fraction of ∼12%, the size of the TiB_2 and their number is small and their effect on crack propagation is minimal. This explains why the fracture toughness and strength are smaller than those for samples containing 8 wt% B_4C addition despite the fact that the level of porosity in samples with 4 wt% B_4C is smaller.

At higher levels of B_4C additions, above approximately (6–8 wt%), the level of porosity is so high that it controls the toughness of the composite and, as a result, the toughness decreases.

Similar behaviour was observed with flexural strength measurements as depicted in Fig. 4. As with fracture toughness, the strength first increases for all volume fractions of up to 18% TiB_2 (6 wt% B_4C), reaching maximum value at ∼18 vol% and then drops as the volume fraction of TiB_2 is increased above ∼18 vol%.

The increase in flexural strength with volume fraction of TiB_2 particles can be the result of density increase, or equivalent porosity decrease, and/or increase in fracture toughness. The effect of porosity on strength can be determined using equation of the form [7]:

$$\sigma = \{\pi\gamma E_o/[D(1-\nu^2)(1+s/R)\}\left\{1+\frac{4V(1-\upsilon^2)}{\pi} \times\left[2(1+s/R)^3+\frac{3}{2(7-5\upsilon)(1+s/R)^2} +\frac{4-5\upsilon}{2(7-5\upsilon)}\right]\right\}^{-1/2} \quad (4)$$

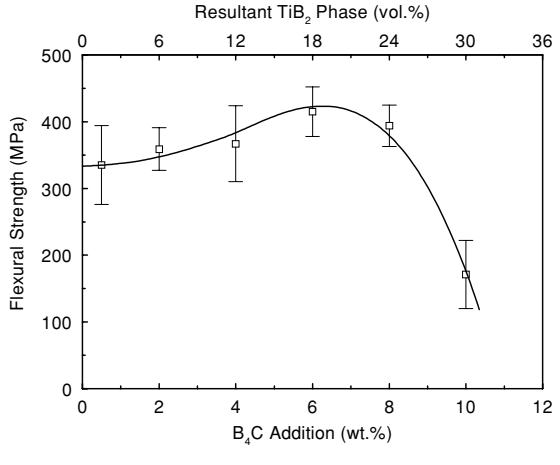

Figure 4 Change of flexural strength of the samples with initial B_4C addition and resultant TiB_2 phase.

TABLE II Relative strength ($(\sigma_f|_v)/(\sigma_f|_{0.5})$) due to change in porosity

	TNBC05	TNBC2	TNBC4	TNBC6	TNBC8	TNBC10
Porosity (%)	5.00	4.13	4.05	5.34	7.48	15.64
Relative strength $((\sigma_f\|_v)/(\sigma_f\|_{0.5}))$	1	1.011	1.012	0.9956	0.9691	0.8847

where γ is the fracture surface energy, E_o is the pore-free Young's modulus, D is the pore diameter ($D = 2R$), R is the pore radius, ν is the Poisson's ratio, s is the annular flow size, and V is the pore volume fraction. Assuming no presence of annular flows ($s/R = 0$), and taking $\nu = 0.2$, the dependence of strength on porosity may be expresses as

$$\sigma \propto \frac{1}{\sqrt{1+3V}}. \quad (5)$$

Using Equation 5, the change of strength of the composite (σ) relative to the strength of samples with 0.5 wt% B_4C ($\sigma_{0.5}$) may be calculated. The results are presented in Table II. Table II shows that the variation of porosity with B_4C addition for up to 6 wt% B_4C (18 vol%) has very small effect on strength of the composite. Only samples with B_4C additions above ∼8 wt% B_4C, which possess high level of porosity, will experience significant decrease in strength. Considering that the change of strength with B_4C follows the same trend as toughness, it is plausible that the increase in fracture strength is governed by the increase in fracture toughness. The general relationship between fracture toughness (K_{IC}) and strength (σ) is given by the equation:

$$K_{IC} = Y\sigma(\pi c)^{1/2} \quad (6)$$

where Y is a dimensional constant which has the value of 1–1.12 and c is the crack size. In order to calculate the change of strength with fracture toughness using Equation 6, one needs to know the value for flaw size c. Careful examination of microstructure of the samples with highest fracture toughness (i.e., samples with 6–8 wt% B_4C additions) reveals that the largest cluster of pores is at the order of 10 μm. The average grain size of the TiN matrix in the same composite is about 9 μm. Substituting values for fracture toughness of 3.5 MPa·m$^{1/2}$ and taking the critical flow size responsible for fracture to be equal to $c = 10 + 5$ μm, Equation 6 gives $\sigma = 455$ MPa. This value for strength is very close to the measured strength of 415 MPa, confirming that the increase in fracture toughness is responsible for the increase in strength. This finding is further reinforced by the flaw size determination in samples with different B_4C additions. Based on measured values for fracture toughness and strength the critical flaw size responsible for fracture can easily be calculated employing Equation 6. The values for the critical flaw size in samples with different B_4C additions are given in Table III. Inspection of Table III shows no significant change in flow size with B_4C addition for all B_4C additions of up to 8 wt%. This is despite large

TABLE III Critical flaw size in samples containing different B_4C additions

B_4C addition (wt%)	2	4	6	8	10
Porosity (%)	4.13	4.05	5.34	7.48	15.64
Critical flaw size (μm)	14.1	14.4	15.0	20.0	56.0

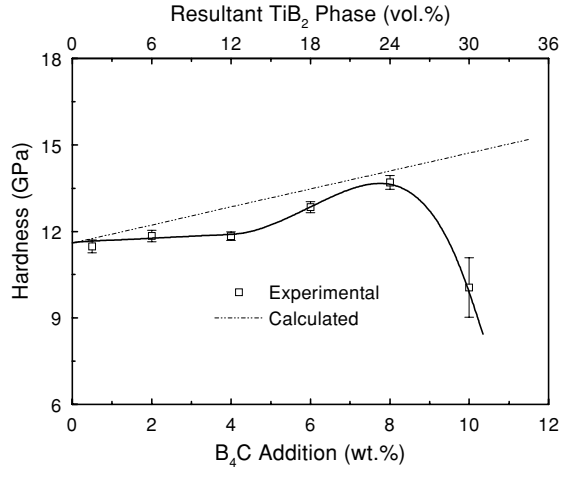

Figure 5 Change of hardness of the samples with initial B_4C addition and resultant TiB_2 phase.

change in grain size of TiN matrix with the change of B_4C addition. For example, the average grain size of the samples with 0.5 wt% B_4C is ~53 μm, whereas that for 6 wt% B_4C is only 9 μm. These results validate the notion that the change of flaw size is not responsible for the increase in flexural strength. Rather, the increase in fracture toughness by crack deflection and residual stresses is the major cause for the increase in flexural strength.

4. Hardness

The variation of hardness with B_4C addition exhibits almost identical trend as the fracture toughness and strength (Fig. 5) do. The hardness value slowly increases from ~11.48 GPa for samples containing 0.5 wt% B_4C to ~13.7 GPa for samples containing 8 wt% B_4C. Above approximately 8 wt% B_4C, the hardness decreased sharply. The hardness value of 13.7 GPa is at the same level as that reported in the literature for the hot-pressed materials [8].

The increase in hardness with B_4C addition is attributed to the increase in volume fraction of TiB_2 particles, which possess significantly higher hardness then the TiN matrix. The reported values for hardness of sintered TiB_2 ceramic varies from 18 to 26 GPa, depending on the purity, grain size and porosity [8]. The TiB_2 particles, in their as-formed state, are relatively small and believed to have almost perfect structure and hardness closer to 26 GPa. Using the rule of mixture and substituting values for hardness of $TiB_2 = 26$ GPa and that of TiN = 11.5 GPa in the following equation

$$H_c = V_{TiB_2} * H_{TiB_2} + V_{TiN} * H_{TiN} \quad (7)$$

the predicted hardness as a function of TiB_2 is obtained as depicted in Fig. 5. Examination of Fig. 5 shows that the measured hardness is somewhat lower than the calculated value, most likely due to the fact that the effect of porosity on hardness was ignored. When porosity is assumed to be a separate phase with zero hardness, excellent agreement between calculated and measured values for hardness is obtained.

5. Conclusions

The reaction sintering of TiN with B_4C addition was found to be highly beneficial not only in increasing the sintered density but also in mechanical properties of the resultant composite. The presence of extremely fine, uniformly distributed particles of TiB_2 serves to pin the TiN grain boundary and enhance all measured mechanical properties. The grain size of the TiN matrix is reduced from 50 μm for samples with 0.5 wt% B_4C addition to only 7 μm for samples with 8 wt% B_4C addition. The fracture toughness increases from 2.68 MPa·$m^{1/2}$ for samples with 2 wt% B_4C (equivalent to 6 vol% TiB_2) to 3.5 MPa·$m^{1/2}$ for samples with 8 wt% B_4C (24 vol% TiB_2). Crack deflection, induced by the hard and high fracture toughness TiB_2 particles, was found to be the major mechanism of toughening. The measured strength was found to increase from 335 MPa for samples with 0.5 wt% B_4C addition to 415 MPa for samples with 6 wt% B_4C (18.2 vol% TiB_2). The increase in toughness was found to be the primary reason for the increase in strength. The increase in hardness from approximately 11.5 GPa for samples with 0.5 wt% B_4C to over 14 GPa for samples with 8 wt% B_4C is due to the presence of much harder TiB_2 particles created during the reaction between TiN and B_4C addition.

References

1. R. W. CHAN, P. HASSEN and E. J. CRAMER, "Materials Science and Technology: A Comprehensive Treatment," Vol. 11 (Structure and Properties of Ceramics, VCH Verlagsgesellshaft mbH, Germany, 1991).
2. T. YAMADA, M. SHIMADA and M. KOIZUMI, *J. Amer. Ceram. Soc.* **59** (1980) 611.
3. K. WANG and V. D. KRSTIC, *Acta Mater.* **51** (2003) 1809.
4. A. G. EVANS and E. A. CHARLES, *J. Amer. Ceram. Soc.* **59** (1976) 371.
5. V. D. KRSTIC, *ibid.* **67** (1984) 589.
6. J. SELSING, *ibid.* **44** (1961) 419.
7. V. D. KRSTIC, *Theoret. Appl. Fract. Mech.* **10** (1988) 241.
8. T. GRAZIANI and A. BELLOSI, *J. Mat. Sci. Lett.* **14** (1995) 1078.

Received 26 September 2002
and accepted 7 July 2003